Cytotoxic responses to 405 nm light exposure in mammalian and bacterial cells: Involvement of reactive oxygen species

Praveen Ramakrishnan [a], Michelle Maclean [a,b], Scott J. MacGregor [b], John G. Anderson [b], M. Helen Grant [a,*]

[a] University of Strathclyde, Department of Biomedical Engineering, Wolfson Centre, 106 Rottenrow, Glasgow, Scotland G4 0NW, United Kingdom
[b] University of Strathclyde, The Robertson Trust Laboratory for Electronic Sterilisation Technologies, 204 George street, Glasgow, Scotland G1 1XW, United Kingdom

ARTICLE INFO

ABSTRACT

Light at wavelength 405 nm is an effective bactericide. Previous studies showed that exposing mammalian cells to 405 nm light at 36 J/cm^2 (a bactericidal dose) had no significant effect on normal cell function, although at higher doses (54 J/cm^2), mammalian cell death became evident. This research demonstrates that mammalian and bacterial cell toxicity induced by 405 nm light exposure is accompanied by reactive oxygen species production, as detected by generation of fluorescence from 6-carboxy-2′,7′-dichlorodihydrofluorescein diacetate. As indicators of the resulting oxidative stress in mammalian cells, a decrease in intracellular reduced glutathione content and a corresponding increase in the efflux of oxidised glutathione were observed from 405 nm light treated cells. The mammalian cells were significantly protected from dying at 54 J/cm^2 in the presence of catalase, which detoxifies H_2O_2. Bacterial cells were significantly protected by sodium pyruvate (H_2O_2 scavenger) and by a combination of free radical scavengers (sodium pyruvate, dimethyl thiourea (•OH scavenger) and catalase) at 162 and 324 J/cm^2. Results therefore suggested that the cytotoxic mechanism of 405 nm light in mammalian cells and bacteria could be oxidative stress involving predominantly H_2O_2 generation, with other ROS contributing to the damage.

1. Introduction

Violet-blue light in the region of 405 nm has antimicrobial activity against a variety of medically-relevant bacterial species (Bache et al., 2012; Maclean et al., 2009, 2013, 2015; McKenzie et al., 2014; Ramakrishnan et al., 2014) and studies have demonstrated increased susceptibility of bacterial cells compared to their mammalian counterparts — potentially providing the ability to preferentially inactivate microbial contamination in wound and tissue environments (Dai et al., 2013; Zhang et al., 2014).

The mechanism of the bactericidal action, and the occurrence of mammalian cell toxicity beyond a threshold exposure level (Ramakrishnan et al., 2014), has not been fully elucidated, but it is thought to involve the photo-excitation of endogenous porphyrin molecules, a process which generates reactive oxygen species (ROS). ROS, including singlet oxygen ($^1O_2$), superoxide anion ($O_2•^-$), hydrogen peroxide (H_2O_2) and hydroxyl groups (•OH), are chemically reactive free radicals that play a crucial role in cell signaling and homeostasis, but overproduction becomes toxic to cells and alters redox balance causing significant damage to cell structures via oxidation of cellular macromolecules such as proteins, lipids, nucleic acids, NADH/NADPH and soluble thiols (Devasagayam et al., 2004). Since mammalian and bacterial cells contain intracellular porphyrins, during violet-blue light exposure, these porphyrins may become photosensitized leading to an overproduction of ROS (Kotelevets et al., 1988; Lavi et al., 2004; Lubart et al., 2011).

As with traditional photodynamic inactivation reactions, which involve the use of exogenous photosensitive dyes or porphyrins (Gayl, 2001), photosensitization using violet-blue light is thought to cause cellular damage via two different pathways: Type I and Type II. With the Type I mechanism, the electronically excited sensitizer (e.g. endogenous porphyrin) reacts directly with the cellular component resulting in free radical formation (e.g. $O_2•^-$ and •OH). These free radicals propagate further free radical chain reactions. In the Type II process, the excited photosensitizer reacts directly with molecular oxygen resulting in the formation of $^1O_2$ (Pattison and Davies, 2006). Both pathways culminate in significant oxidative damage to exposed cells.

The experiments described in this paper were carried out to investigate and compare the inactivation mechanism which occurs within mammalian and bacterial cells upon exposure to toxic levels of 405 nm violet-blue light. The study aimed to demonstrate ROS generation in mammalian and bacterial cells as a consequence of 405 nm violet-blue light exposure, and also to determine whether these ROS

---

* Corresponding author at: University of Strathclyde, Department of Biomedical Engineering, Wolfson Centre, 106 Rottenrow, Glasgow, Scotland G4 0NW, United Kingdom.

E-mail address: m.h.grant@strath.ac.uk (M.H. Grant).

contributed to its cytotoxicity. With 405 nm light being highlighted in a number of recent studies as having potential applications for patient-safe environmental decontamination and wound decontamination, determining the effects induced in mammalian and bacterial cells upon exposure is important (Maclean et al., 2010; McDonald et al., 2011).

Osteoblasts, and the bacterium *Staphylococcus epidermidis*, were selected for use in this study as an example of a robust mammalian cell type, and a component of the natural skin microflora and common cause of hospital infection, respectively (Cogen et al., 2008; Waugh and Lawrence, 2013; Otto, 2009). Both cell types have also previously been investigated for their susceptibility to 405 nm light (McDonald et al., 2011, 2013; Ramakrishnan et al., 2014). In the present study, cells were exposed to increasing doses of 405 nm light to study how this affected the production of intracellular ROS in both the mammalian and bacterial cells. Oxidation (dimerization) of glutathione (GSH) to oxidised glutathione (GSSG) was utilised as an indicator of oxidative stress in mammalian cells (Engelmann et al., 2005). In order to detect and measure the production of intracellular ROS in mammalian and bacterial cells, 6-carboxy-2′, 7′-dichlorodihydrofluorescein diacetate dye (carboxy-H_2DCFDA) was chosen. Carboxy-H_2DCFDA is a chemically reduced, acetylated form of fluorescein used as an indicator for ROS in cells including cancer cells, astrocytes and phagocytes (Brubacher and Bols, 2001; Testa et al., 2011; Trifunovic et al., 2005; Wu and Yotnda, 2011). This non-fluorescent molecule is readily converted to a green-fluorescent form when the acetate groups are removed by intracellular esterases, and oxidation by interaction with ROS occurs within the cell. The generation of green fluorescence from carboxy-H_2DCFDA following de-acetylation and oxidation is indicative of the presence of oxidative stress (Johnson and Spence, 2010). The cytotoxic response to the 405 nm light exposure was monitored by the reduction of (3-(4,5-dimethylthiazol-2-yl)-2,5-diphenyltetrazolium bromide) (MTT), which correlates cell metabolic activity with viability. The osteoblasts are an adherent cell line, and the number of viable cells adhering to the culture dishes after exposure to the light was also monitored by total cell protein.

In order to further evaluate the role of ROS in the cytotoxic mechanism, ROS scavengers, which can aid in cell protection by either preventing or removing the excess ROS produced during oxidative stress conditions, were used (Sies, 1997). Sodium pyruvate (an intracellular H_2O_2 scavenger), dimethyl thiourea (DMTU, an intracellular •OH scavenger) and catalase (detoxifies extracellular H_2O_2) were added to mammalian and bacterial cell samples, both singly and in combination, during 405 nm light exposure, and the effect on the cells monitored. These scavenging chemicals were chosen based on their successful use in a previous study by MacLean and co-workers (Maclean et al., 2008). Sodium pyruvate has previously been shown to protect human neuroblastoma cells at concentrations ≥1 mM against H_2O_2 insult (Wang et al., 2007), and DMTU, an •OH scavenger, effectively protects renal cells and human bronchial epithelial cells at concentrations of 1 mM (Linas et al., 1987) and 10 mM (Rappeneau et al., 2000) respectively. Preliminary experiments with each of the scavengers were carried out to determine the effective dose, and ascertain that they were not toxic to the cells at that dose. The study results are discussed in terms of the cellular mechanisms involved in 405 nm violet-blue light cellular inactivation, and factors influencing the differing susceptibility of mammalian and bacterial cells to the light.

2. Materials and methods

2.1. Culture and 405 nm light exposure of mammalian cells

Immortalised osteoblast (OST 5) cells isolated by SV40 transfection of neonatal rat calvarial osteoblasts in our laboratory and used previously in toxicity experiments (Ramakrishnan et al., 2014) were cultured as monolayers using Dulbecco's Modified Eagle's Medium (DMEM) containing 10% v/v foetal calf serum in an atmosphere of 5% CO_2 in air at 37 °C.

The 405 nm light system used in this study consisted of an array of nine 405 nm light emitting diodes (LEDs) (GE Illumination, USA), with a full-width half-maximum of 14 nm. The LEDs were arranged in a 3×3 grid pattern (6 cm × 6 cm), and attached to a heat sink for thermal management, thus preventing sample heating during light exposure. The heat sink was supported by two pillars above a moulded base designed to fit a multi-well plate in order to fix the position of the treatment plates directly below the LEDs. The light source was set at a height of 8 cm above the multi-well plate, and the middle 4 wells in a 24-well plate, and the middle 16 wells in a 96-well plate, were used for cell exposures. Cells were seeded at a density of 5×10^3 cells/cm^2 in 24-well plates, and 2×10^4 cells/cm^2 in 96-well plates, and left in the incubator overnight at 37 °C.

Post-incubation, growth medium was removed and 1 ml Dulbecco's Phosphate Buffered Saline (DPBS) solution was added to the central wells. The plates were transferred to an incubator at 37 °C and 5% CO_2 where the samples were exposed to increasing doses of 405 nm light (Table 1), with dose (J/cm^2) calculated as the product of the irradiance (W/cm^2) × time (s). Unexposed controls were held under the same conditions but in a separate incubator (to avoid any effects of the light on the control). After the stipulated exposure periods, the following assays were performed on both the light-exposed and non-exposed control samples.

2.2. ROS detection and measurement in mammalian cells

ROS detection and measurement in adherent osteoblast cells were carried out using 6-carboxy-2′,7′-dichlorodihydrofluorescein diacetate (carboxy-H_2DCFDA) dye (Invitrogen, UK: C400, Lot 28351W). After 405 nm light treatments at 5 mW/cm^2 for 1, 1.5, 2, 2.5 and 3 h (18, 27, 36, 45 and 54 J/cm^2 respectively), the DPBS solution was removed from the wells, and the cell monolayer washed twice with DPBS. The washing step was used to remove any cell debris present in the sample after 405 nm light exposure. The samples were immediately treated with 200 μl of 25 μM carboxy-H_2DCFDA and incubated in the dark at 37 °C for 30 min to allow the probe to accumulate within the cells. After incubation, the cells were washed twice with DPBS. 1 ml 0.1% (v/v) Triton X-100 was then added to each well, and the cells incubated in the dark at room temperature for 20 min to allow the fluorochrome to leach out of the cells. Fluorescence was measured immediately using a RF-5001PC spectrofluorophotometer at an excitation wavelength of 495 nm and emission wavelength of 525 nm as described previously (Smith et al., 1992).

For microscopic imaging, cells (5×10^3 cells/cm^2) were grown on coverslips placed in the wells of 24-well plates. Post-light treatment, cells were washed twice with DPBS, 200 μl of 25 μM carboxy-H_2DCFDA was added to the cells and they were then incubated in the dark at 37 °C for 30 min. Post-incubation, excess dye was removed, cells were washed twice with DPBS, coverslips were placed onto microscopic slides and the samples viewed under a Axio Imager Z1 fluorescent microscope (Zeiss, Hertfordshire, UK) for green fluorescence at an excitation wavelength of 450–490 nm and emission wavelength of 515–565 nm using a 20× water lens (NA = 0.5).

Table 1
The different periods of osteoblast cell exposure to 405 nm light, irradiance levels and the corresponding applied doses.

Exposure period (hours)	Irradiance (mW/cm^2)	Dose (J/cm^2)
1	5	18
1.5	5	27
2	5	36
2.5	5	45
3	5	54

2.3. Extracellular oxidised glutathione (GSSG) and intracellular reduced glutathione (GSH) measurement

After 405 nm light treatment at 5 mW/cm^2 for 0, 1, 1.5, 2, 2.5 and 3 h (0, 18, 27, 36, 45 and 54 J/cm^2 respectively), 800 μl of DPBS buffer was removed from the wells without detaching the cells. The buffer was centrifuged at 10,000 ×g for 2 min to remove cell debris. 200 μl of 25% (w/v) trichloroacetic acid (TCA) was then immediately added to the centrifuged supernatants (to prevent any further oxidation of GSH to GSSG) and extracellular GSSG measured using N-ethylmaleimide (NEM), O-phthalaldehyde (OPT) and 0.2 M sodium hydroxide (NaOH) as described previously (Hissin and Hilf, 1976), at 350 nm excitation and 420 nm emission using a RF-5001PC spectrofluorophotometer (Shimadzu, Japan).

200 μl of 10% (w/v) TCA was then added to the cells and the plates were placed on ice for 10 min. Thereafter, GSH was measured in the cellular acidic extracts using OPT as described previously (Hissin and Hilf, 1976), at 350 nm excitation and 420 nm emission using a RF-5001PC spectrofluorophotometer.

The loss in intracellular GSH (in nmol/ml) was correlated with the gain in extracellular GSSG in the buffer (taking into account differences in the volumes of the samples), between samples treated with 45 and 54 J/cm^2 to determine whether GSH loss was due to oxidation.

2.4. Measurement of mammalian cell viability in the presence and absence of scavengers

Cells were seeded at 5×10^3 cells/cm^2 in 24 well plates prior to exposure. The osteoblasts were exposed to 54 J/cm^2 405 nm light treatment (5 mW/cm^2 for 3 h) in the absence and presence of reactive oxygen species (ROS) scavengers: sodium pyruvate (1 mM,), dimethyl thiourea (1 mM,) and catalase (50 U/ml). The total protein content of the osteoblasts was determined 2 days after exposure and after solubilising the cells in 0.5 M NaOH overnight (Lowry et al., 1951). Mammalian cell viability was measured using the MTT assay as described previously (Ho et al., 2004). For each scavenger used, appropriate non-exposed controls were included in each experiment.

2.5. Culture and 405 nm light treatment of bacterial cells

S. epidermidis LMG 10474 (Laboratorium voor Microbiologie, Universiteit Gent, Belgium) was inoculated in 100 ml nutrient broth (NB) and incubated at 37 °C for 18 h under rotary conditions (120 rpm). Post-incubation, the broth was centrifuged at 3939 ×g for 10 min, and the pellet re-suspended in 100 ml PBS, giving a population density of approximately 10^9 colony forming units (CFU)/ml. 2 ml suspension was transferred into the middle 2 wells of a 12-well plate and exposed, at room temperature, to increasing doses of 405 nm light (Table 2). Unexposed controls were held under the same conditions but without 405 nm light exposure.

2.6. ROS detection and measurement in bacterial cells

After 405 nm light treatments at 15 mW/cm^2 for 0, 1, 3 and 6 h (0, 54, 162 and 324 J/cm^2 respectively), the bacterial cell suspensions

were removed from the wells, and centrifuged at 3939 ×g for 10 min to achieve a cell pellet. 200 μl 25 μM carboxy-H$_2$DCFDA was then added to the pellet, mixed, and left in the dark for 30 min at room temperature. Post-incubation, 195 μl of the aliquot was made up to 1 ml with PBS, and the fluorescence measured as described for the mammalian cells, directly in the cell suspension.

For microscopic imaging, 5 μl of the undiluted pellet with dye was pipetted onto a microscope slide and viewed for green fluorescence as described for the mammalian cells, but using a 100× oil immersion lens (NA = 0.5).

2.7. Detection and measurement of bacterial ROS in the presence of scavengers

The bacterial cell suspensions were exposed to 162 J/cm^2 405 nm light (15 mW/cm^2 for 3 h) in the presence of the reactive oxygen species scavengers (100 mM Sodium pyruvate; 100 mM Dimethyl thiourea; 200 U/ml catalase). After light treatment, the bacterial cell suspensions were removed from the wells, and the fluorescence measured fluorimetrically and detected microscopically using carboxy-H$_2$DCFDA as described earlier. For each scavenger used, appropriate non-exposed controls were included in each experiment.

2.8. Measurement of bacterial cell viability in the presence and absence of ROS scavengers

After exposure of bacterial suspensions to 15 mW/cm^2 405 nm light for 3 and 6 h (162 and 324 J/cm^2 respectively), bacterial samples were diluted in PBS, plated onto nutrient agar (NA), and incubated at 37 °C overnight before enumeration of the viable CFU/ml. To assess the effect of ROS scavengers on the inactivation kinetics, exposures were repeated in the presence of a range of scavengers: 100 mM Sodium pyruvate; 100 mM dimethyl thiourea; and 200 U/ml catalase, both individually, and combined (at the same concentrations). For each scavenger used, appropriate non-exposed controls were included in each experiment.

3. Results

3.1. ROS detection in mammalian cells using carboxy-H$_2$DCFDA

The green fluorescence generated from carboxy-H$_2$DCFDA was detected by both fluorescence microscopy (Fig. 1A), and by quantitative fluorescence measurement by spectrofluorimetry of the lysed cells (Fig. 1B). The fluorescence intensity measurement for the unexposed bar (Fig. 1B) was averaged over all exposure time points. This procedure was justified because there was no significant difference between the unexposed samples at all time points (p > 0.05), using one-way ANOVA plus Tukey post hoc test. Data in Fig. 1A and B show a significant increase (p < 0.05) in intracellular green fluorescence for 405 nm light treated samples for up to a period of 2 h (36 J/cm^2) when compared with the respective unexposed samples, using one-way ANOVA plus Dunnett's post-hoc test. The intracellular fluorescence of the 405 nm treated cells decreased at 2.5 and 3 h exposures (45 and 54 J/cm^2) compared to 2 h exposed samples.

3.2. Measurement of GSH/GSSG content in mammalian cells

The intracellular GSH content of, and the GSSG efflux from, the mammalian cells were measured post-405 nm light treatment at different doses to find out whether the cells experienced oxidative stress. Data in Fig. 2 show that there was a significant decrease (p < 0.05) in the intracellular GSH content of the light-exposed cells at 3 h (54 J/cm^2) compared with the respective unexposed samples. There was no significant decrease in GSH levels prior to this dose. The extracellular GSSG concentration of the light-exposed samples increased significantly at 3 h exposure (54 J/cm^2) (p < 0.05) when compared with their respective unexposed

Table 2
The different periods of bacterial cell exposure to 405 nm light, irradiance levels and the corresponding applied doses.

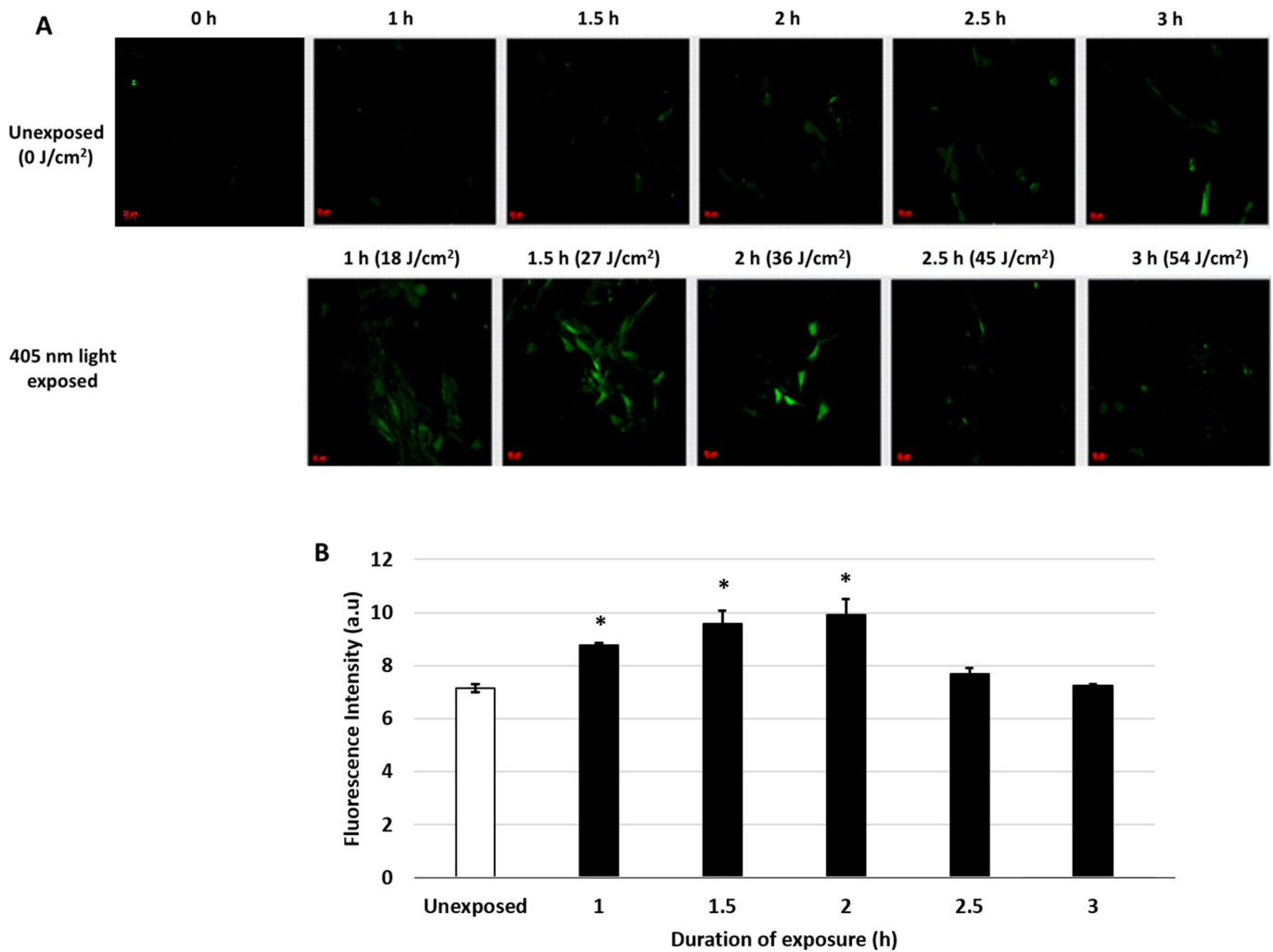| Exposure period (hours)	Irradiance (mW/cm^2)	Dose (J/cm^2)
1	15	54
3	15	162
6	15	324

Fig. 1. Detection of ROS production in immortalised rat osteoblasts upon exposure to 5 mW/cm^2 405 nm light for 1, 1.5, 2, 2.5 and 3 h (18, 27, 36, 45 & 54 J/cm^2 respectively), using carboxy-H$_2$DCFDA. (A) Visual detection using fluorescence microscopy at an excitation wavelength of 450–490 nm and emission wavelength of 515–565 nm and (B) measurement of fluorescence intensity at an excitation wavelength of 495 nm and emission wavelength of 525 nm. Data (Mean ± SEM, n = 4 independent experiments and all samples were duplicated in each experiment) were analysed using one-way ANOVA plus Dunnett's post-hoc test. * indicates a significant difference (p < 0.05) between light-exposed and unexposed samples.

samples (Fig. 2). The amount of intracellular GSH lost from the cells (nmol) was accounted for by the gain in extracellular GSSG (nmol). Taking the data from those presented on Fig. 2, 0.21 ± 0.02 nmol of GSH lost from the cells were accounted for by a gain of 0.09 ± 0.03 nmol GSSG in the extracellular buffer between exposure periods of 2.5 and 3 h (45 and 54 J/cm^2 respectively).
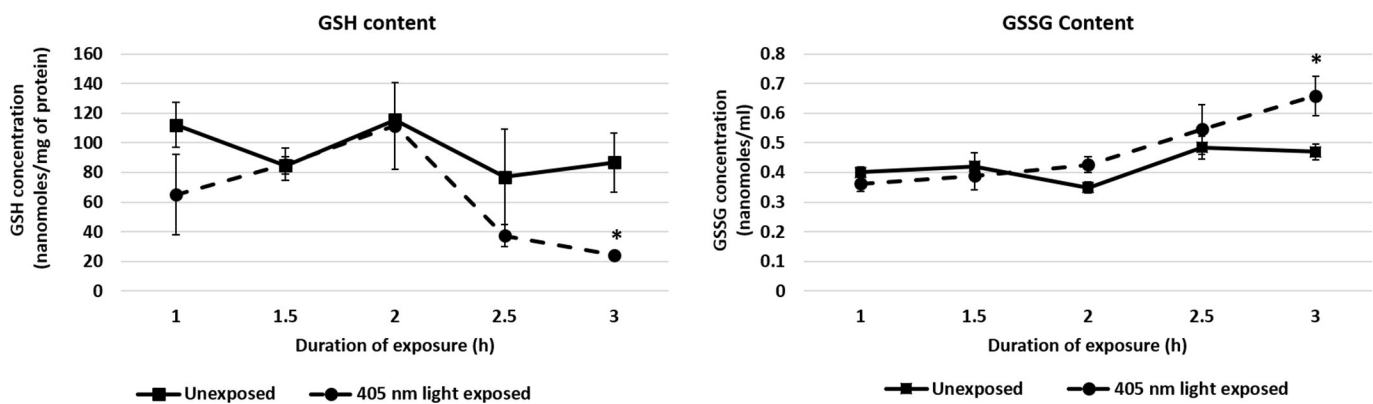

Fig. 2. Intracellular GSH concentration and extracellular GSSG concentration of rat osteoblasts exposed to 5 mW/cm^2 405 nm light for 1, 1.5, 2, 2.5 and 3 h (18, 27, 36, 45 & 54 J/cm^2 respectively). Data (Mean ± SEM, n = 4 independent experiments and all samples were duplicated in each experiment) were analysed using unpaired Student's t-test; * indicates a significant difference (*, p < 0.05) between light-exposed and unexposed samples.
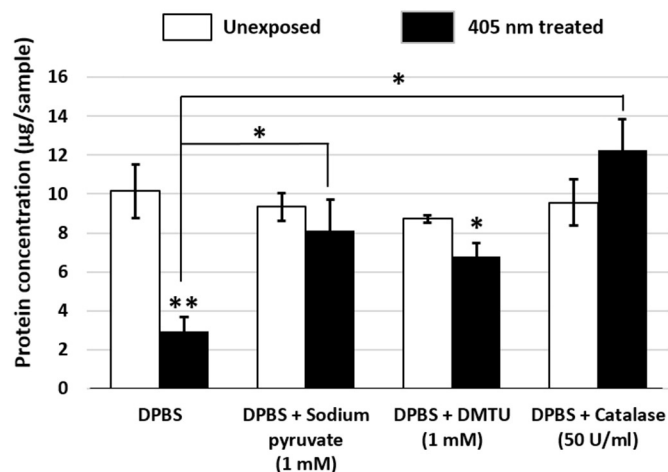
Fig. 3. Protein concentration of rat osteoblasts exposed to 5 mW/cm² 405 nm light at a dose of 54 J/cm² (3 h exposure), in the absence (DPBS alone) and presence of ROS scavengers: sodium pyruvate (1 mM), DMTU (1 mM) and catalase (50 U/ml). Measurements were made 48 h post-treatment. Data (Mean ± SEM, n = 4 independent experiments and all samples were duplicated in each experiment) were analysed using an unpaired Student's t-test to detect significant differences between light-exposed and unexposed samples; (*, p < 0.05; **, p < 0.001) and one-way ANOVA plus Dunnett's post-hoc test to detect significant differences between light-exposed samples in the presence and absence of scavengers (*, p < 0.05, denoted by line connectors).

Fig. 4. % of cellular MTT reduction of rat osteoblasts exposed to 5 mW/cm² 405 nm light at a dose of 54 J/cm² (3 h exposure), in the absence (DPBS alone) and presence of ROS scavengers: sodium pyruvate (1 mM), DMTU (1 mM) and catalase (50 U/ml). Control taken as 100%, is unexposed cells treated with or without individual scavengers. Measurements were made 48 h post-treatment. Data (Mean ± SEM, n = 3 independent experiments and all samples were quadrupled in each experiment) were analysed using an unpaired Student's t-test to detect significant differences between light-exposed and unexposed samples (**, p < 0.01; ***, p < 0.001); and one-way ANOVA plus Dunnett's post-hoc test to detect significant differences between light-exposed samples in the presence and absence of scavengers (*, p < 0.05, denoted by line connectors).

3.3. Mammalian cell viability in the presence and absence of ROS scavengers

Having shown generation of elevated ROS levels in both mammalian and bacterial cells during exposure to 405 nm light, experiments were carried out to find out whether or not cell viability was affected, and whether free radical scavengers could offer cell protection. Data in Fig. 3 show significantly decreased protein content for 405 nm light-treated samples exposed for 3 h (54 J/cm²) in DPBS alone (p < 0.001), compared with the unexposed control. Interestingly, there was no significant decrease in protein content of the samples exposed to the same dose in the presence of sodium pyruvate (1 mM) and catalase (50 U/ml), compared with their respective unexposed controls. This demonstrates that the sodium pyruvate and catalase were able to prevent the loss of protein observed in non-scavenger exposed cells exposed to 405 nm light for 3 h. DMTU did not protect the light exposed cells when compared to either the cells exposed in the absence of scavengers (p > 0.05), or unexposed DMTU treated control cells (p > 0.05).

When light toxicity was measured in terms of % of cellular metabolic activity (Fig. 4), only catalase offered complete protection from the effects of 405 nm light. In the presence of both sodium pyruvate and DMTU the toxicity of the light was evident by the decrease in % of cellular metabolic activity.

3.4. ROS detection in bacterial cells using carboxy-H₂DCFDA

In the bacteria, the accumulation of fluorescence is also shown both by microscopic images (Fig. 5A) and by quantitative spectrofluorimetry (Fig. 5B). The fluorescence intensity measurement for the unexposed bar (Fig. 5B) was averaged over all exposure time points. This procedure was justified because there was no significant difference between the unexposed samples at all time points (p > 0.05), using one-way ANOVA plus Tukey post hoc test. Data in Fig. 5A & B show a significant increase in green fluorescence in 405 nm light-treated samples at exposure periods of 1 and 3 h (54 J/cm² and 162 J/cm² respectively) when compared with their respective controls, using one-way ANOVA plus Dunnett's post-hoc test. The green fluorescence of 405 nm treated
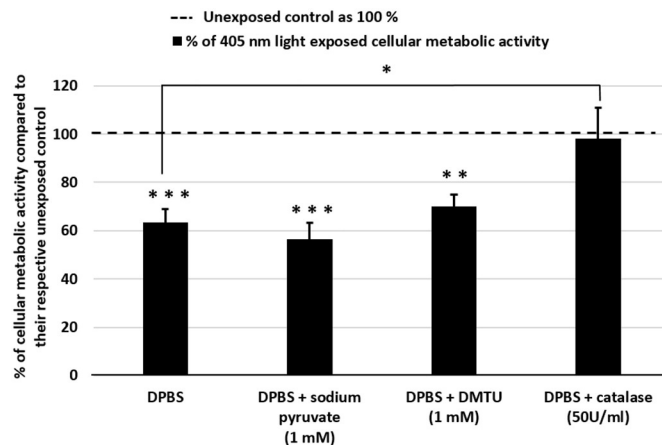
samples decreased at an exposure period of 6 h (324 J/cm²) compared to the 3 h (162 J/cm²) exposed samples.

3.5. ROS detection and measurement in bacterial cells in the presence of scavengers using carboxy-H₂DCFDA

To check for a decrease in ROS production in bacterial cells in the presence of scavengers, carboxy-H₂DCFDA was used. A dose of 162 J/cm² (15 mW/cm² for 3 h) was selected for use as it was the mid-point on the inactivation curve (Fig. 7). Data show, both visually (Fig. 6A) and spectroscopically (Fig. 6B), that least increase in fluorescence is produced with the cells exposed in the presence of sodium pyruvate and the scavenger combination, which correlates well with the cell viability results (Fig. 7).

3.6. Bacterial cell viability in the presence and absence of ROS scavengers

Exposure of *S. epidermidis* to 405 nm light in the absence of scavengers produced significant population reductions (Fig. 7), with a 4.8-log₁₀ reduction at an exposure period of 3 h (162 J/cm²) (p < 0.001), increasing to a 7-log₁₀ reduction by 6 h (324 J/cm²) (p < 0.001). Due to the high (10⁹ CFU/ml) population density used, higher concentrations of ROS scavengers than those used for the mammalian cell study (100 mM sodium pyruvate, 100 mM DMTU), 200 U/ml catalase) were used to investigate whether they exerted a protective effect on bacterial cells exposed to 405 nm light. Results showed that when cells were exposed in the presence of sodium pyruvate, bacterial inactivation was significantly reduced, with only 2.8-log₁₀ reduction achieved after a 3 h exposure period: 2-log₁₀ less than in the absence of scavengers. A degree of protection was observed with catalase, with 1.1-log₁₀ less inactivation at 3 h, than in the absence of scavengers (p < 0.05), however, by 6 h, the bacterial population had decreased to a similar level as measured without scavengers. DMTU appeared to offer no protection to 405 nm light-exposed cells at the concentration used in this study. Interestingly, the greatest protection was afforded by the combined use of the three scavengers, with inactivation at 3 h reduced by 3.5 log₁₀ compared to that in the absence of scavengers (p < 0.05). By 6 h, protection from the scavenger combination was similar to that exerted by the sodium pyruvate.
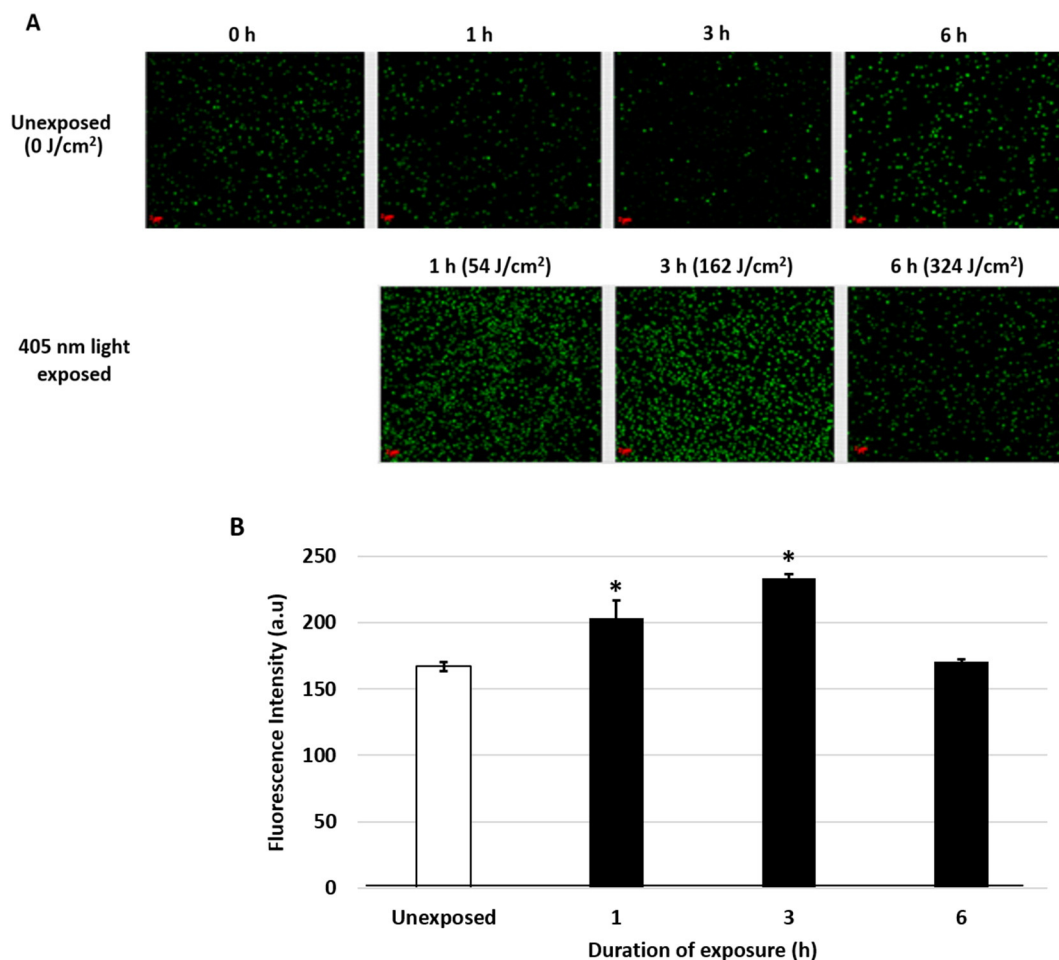
Fig. 5. Detection of ROS production using carboxy-H_2DCFDA in the bacterium *Staphylococcus epidermidis*, at a population of 10^9 CFU/ml, upon exposure to 15 mW/cm^2 405 nm light for 1, 3 and 6 h (54, 162, 324 J/cm^2 respectively). (A) Visual detection using fluorescence microscopy at an excitation wavelength of 450–490 nm and emission wavelength of 515–565 nm and (B) measurement of fluorescence intensity at an excitation wavelength of 495 nm and emission wavelength of 525 nm. Data (Mean ± SEM, n = 3 independent experiments and all samples were duplicated in each experiment) were analysed using one-way ANOVA plus Dunnett's post-hoc test. * indicates a significant difference (p < 0.05) between light-exposed and unexposed samples.

4. Discussion

While investigating the effects of 405 nm light on normal function, proliferation rate and viability of rat osteoblasts, it was found that an exposure period of more than 2 h at an irradiance level of 5 mW/cm^2 (>36 J/cm^2) was toxic to cells leading to an impairment in cell function and cell death (Ramakrishnan et al., 2014). Hence, the mechanism(s) responsible for cell kill by 405 nm light were sought to find out whether oxidative stress was involved. Glutathione exists in both reduced (GSH) and oxidised (GSSG) states. The ratio of reduced to oxidised glutathione within cells is often used as a marker of cellular toxicity (Carelli et al., 1997; Locigno and Castronovo, 2001; Noctor and Foyer, 1998; Townsend et al., 2003) and an increase in GSSG concentration has been reported to be an indicator of oxidative stress (Aukrust et al., 1995). GSSG is expelled from cells rapidly and accumulates extracellularly.

When oxidative stress occurs within a cell, excessive production of ROS overwhelms the cellular antioxidant defence systems. Enhanced production of ROS in the cells leads to lipid peroxidation, protein and nucleic acid oxidation, enzyme inhibition and activation of programmed cell death pathway, ultimately causing cell death (Sharma and Dubey, 2005; Meriga et al., 2004; Mittler, 2002; Shah et al., 2001). During photosensitization of the cell, it is thought that the porphyrin molecules present within the cell absorb light energy and become excited from the singlet ground state, to a singlet excited state, which then undergoes intersystem crossing to the triplet state (Chiaviello et al., 2011). The

excited photosensitizer can then react with either ground state triplet oxygen to form excited state singlet oxygen ($^1O_2$), or with cell components to form free radicals and radical ions. The half-life of some of these free radicals is in the range of 10^{-6} ($O_2^{\bullet-}$ and $^1O_2$) to 10^{-9} s (•OH).

A significant increase in green fluorescence for the 405 nm treated samples for up to an exposure period of 2 h, clearly indicates that there was an overproduction of ROS present (Fig. 1). One of the reasons for the reduction of green fluorescence within the 405 nm treated cells at 2.5 and 3 h, compared to the 2 h exposed samples, could be due to the cells dying. The dying cells would have damaged membranes, and as a result intracellular esterases would be lower in concentration, resulting in less deacetylation of the non-fluorescent dye molecule, and furthermore the fluorescent dye formed could escape from the cells. Alternatively, there is also a possibility that the cells might have upregulated their intrinsic antioxidant capacities, counteracting the increased ROS formation at high doses of 405 nm light exposure i.e. 2.5 and 3 h. However from our earlier study on mammalian cell viability post-405 nm light exposure (Ramakrishnan et al., 2014), there was a significant reduction in cell viability, function and proliferation rate in 405 nm light exposed samples at 2.5 and 3 h, after a 48 and 72 h post-treatment period. This also suggests that the reduction in green fluorescence observed at higher exposure periods of 405 nm light is likely due to the cells dying.

Experiments measuring the GSH/GSSG concentration of mammalian cells were carried out post-405 nm light treatment at different time
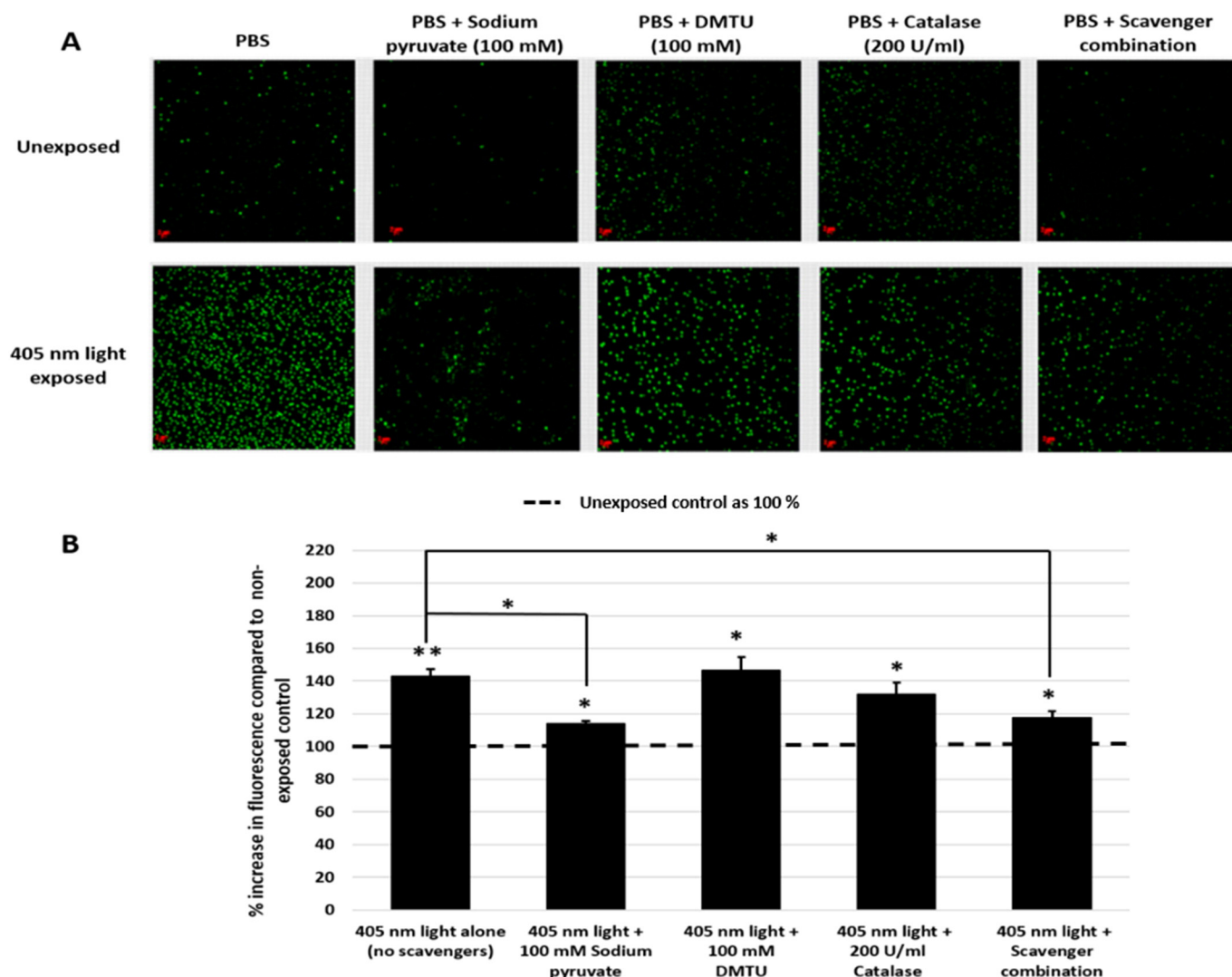
A

B

Fig. 6. Detection of ROS production in *Staphylococcus epidermidis*, at a population of 10^9 CFU/ml, exposed to 162 J/cm^2 405 nm light (15 mW/cm^2 for 3 h) in the absence (in PBS) and presence of ROS scavengers, using carboxy-H$_2$DCFDA. The scavengers used were: 100 mM sodium pyruvate, 100 mM DMTU, 200 U/ml catalase, and a combination of the three (at the same concentrations). (A) Visual detection using fluorescence microscopy at an excitation wavelength of 450–490 nm and emission wavelength of 515–565 nm and (B) measurement of % increase in fluorescence intensity compared to non-exposed control, at an excitation wavelength of 495 nm and emission wavelength of 525 nm. Control taken as 100% is unexposed cells treated with or without scavengers. Data (mean ± SEM, n = 3 independent experiments and all samples were duplicated in each experiment) were analysed using an unpaired Student's t-test to detect significant differences between light-exposed and unexposed samples (*, p < 0.05; **, p < 0.001); and using one-way ANOVA plus Dunnett's post-hoc test to detect significant differences between light-exposed sample in the presence and absence of scavengers (*, p < 0.05, denoted by line connectors).

periods ranging from 1–3 h. In Fig. 2, the results showed a significant decrease in intracellular GSH concentration and a significant increase in extracellular GSSG production at 3 h for the 405 nm treated samples, thus indicating oxidative stress in the cells.

Normally, cells defend themselves against ROS damage with enzymes such as catalases, superoxide dismutases and glutathione peroxidases, and antioxidants such as α-tocopherol, ascorbic acid, uric acid and glutathione (Ames et al., 1981; Faraci and Didion, 2004; Li et al., 1995; Packer et al., 2001; Padayatty et al., 2003; Pompella et al., 2003; Tanaka et al., 2002). In order to find out whether scavengers, when added externally to cells, limited the toxic effects of ROS and provided cell protection, sodium pyruvate (a H$_2$O$_2$ scavenger) (Desagher et al., 1997), DMTU (a •OH scavenger) (Bruck et al., 2001) and catalase (detoxifies H$_2$O$_2$) (Schimmel and Bauer, 2002) were added to mammalian cells during 405 nm light treatment. Figs. 3 and 4 show that after a dose of 54 J/cm^2 (5 mW/cm^2 for 3 h) and a 48 h post-treatment period, 50 U/ml catalase offered complete protection to 405 nm treated osteoblasts. Hockberger et al. (1999) also showed that light in the violet-blue region led to ROS formation in mammalian cells, especially H$_2$O$_2$, and that catalase was protective against this H$_2$O$_2$ insult (Hockberger et al., 1999). It is known that

H$_2$O$_2$, which is produced from O$_2$•$^-$ by the action of superoxide dismutase, is relatively stable and can last for many seconds within the cell, so it is likely to exert significant effects on the cellular biochemistry in that time. However, it is also highly permeable to cell membranes, and may have been released from the cells, which would explain why extracellular catalase can be cytoprotective although it does not penetrate the cell membrane. In this study sodium pyruvate which is also a H$_2$O$_2$ scavenger, did show a protective effect towards 405 nm treated samples when investigating protein concentration but did not have a cytoprotective effect at 1 mM (or at 10 mM (data not shown)) in terms of % cellular metabolic activity. From the literature it is suggested that pyruvate at similar concentrations causes acidification of cell cytosol. If cytosolic pH is reduced, this will affect the ability of reductase enzymes to reduce MTT, possibly accounting for a decrease in MTT reduction. No such decrease in attached viable cells measured by protein was observed after treatment with pyruvate, indicating that the decrease in pH is sub-lethal (Desagher et al., 1997). DMTU, did not significantly protect the cells from dying, possibly due to the short half-life (10^{-9} s) of •OH radicals.

As with the damage to mammalian cells, the bactericidal effect of 405 nm light (Bache et al., 2012; Maclean et al., 2009, 2013, 2015;

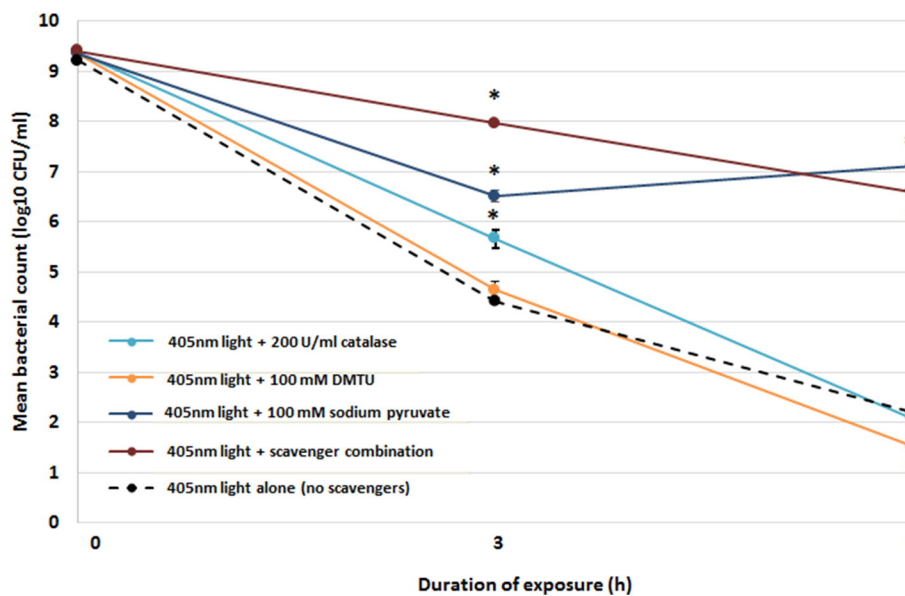**Fig. 7.** Viability of *Staphylococcus epidermidis* exposed to 15 mW/cm^2 405 nm light for 3 and 6 h (162 & 324 J/cm^2) in the absence (in PBS) and presence of ROS scavengers: 100 mM sodium pyruvate, 100 mM DMTU, and 200 U/ml catalase. Bacteria were also exposed to a combination of the scavengers, at the same concentrations. Data (mean log$_{10}$ CFU/ml ± SEM, n = 4 independent experiments and all samples were duplicated in each experiment) were analysed using a one-way ANOVA plus Dunnett's post-hoc test. * indicates a significant difference (p < 0.05) between light-exposed samples in the presence and absence of scavengers. No significant change was detected in the non-exposed control samples over the duration of the experiment (p > 0.05).

McKenzie et al., 2014; Ramakrishnan et al., 2014) is also thought to be caused by photoexcitation of endogenous porphyrins within the cell leading to the production of ROS. This study aimed to confirm that a similar cytotoxic mechanism exists in mammalian and bacterial cells. To detect ROS production, the DCFDA dye, which has previously been used to detect ROS in bacteria including *Escherichia coli* and *Staphylococcus aureus* (Hwan et al., 2011; Jung et al., 2003), detected an increase in green fluorescence in 405 nm treated bacterial samples after 1 and 3 h exposure periods, thus clearly indicating an overproduction of ROS within the 405 nm treated cells (Fig. 5). The decrease in green fluorescence after an exposure period of 6 h compared to the 3 h exposed sample is again likely due to dying bacterial cells, as observed with the mammalian osteoblasts.

The effectiveness of scavengers on *S. epidermidis* during 405 nm light treatments was studied by measuring viable bacteria (log$_{10}$ CFU/ml) after a 24 h post-treatment period and by spectrofluorometric and microscopic measurement of ROS production. Results showed that bacterial inactivation could be significantly reduced when cells are exposed to the light in the presence of certain scavengers. Sodium pyruvate proved to be the single most effective ROS scavenger, indicating that, as in the case of the mammalian cells, H$_2$O$_2$ is one of the key ROS responsible for bacterial cell death. Catalase offered a degree of protection at the mid-point of the inactivation kinetics, however, possibly due to the concentration used not being sufficient to offer protection against large amounts of intracellular H$_2$O$_2$, it became ineffective at the later point in the inactivation curve. DMTU did not have an effect on cell viability indicating that either •OH caused less toxic damage to cells due to its short life span (10^{-9} s) or the concentration of DMTU used was not sufficient enough to offer any protection. The combined use of the three scavengers offered most protection to the 405 nm exposed bacteria cells, thus suggesting that the different ROS may each exhibit different levels of toxicity and play a role to some extent.

Overall, this study has demonstrated that exposure to toxic levels of 405 nm light induces over-production of ROS in both mammalian and bacterial cells, and that oxidative stress plays a key role in cell death. It was not possible to directly compare the ROS generation and viability of the mammalian and bacterial cells, because for spectrofluorometric analysis and fluorescence microscopy visualisation of the bacteria, the use of significantly higher population densities was required, making

direct comparison of results difficult. These increased bacterial population densities meant that increased doses of 405 nm light needed to be used to exert cell damage, and higher scavenger concentrations were thus needed to investigate of any protective effects.

Nonetheless, despite these limitations, results have clearly demonstrated that the cytotoxic mechanism triggered in both mammalian cells and bacterial cells upon exposure to 405 nm light has distinct similarities, with both processes involving oxidative damage via the production of ROS, with H$_2$O$_2$ appearing to have a key role in cellular damage in both cases.

Transparency document

The Transparency document associated with this article can be found, in the online version.

Acknowledgments

References

Ames, B.N., Cathcart, R., Schwiers, E., Hochstein, P., 1981. Uric acid provides an antioxidant defense in humans against oxidant- and radical-caused aging and cancer: a hypothesis. Proc. Natl. Acad. Sci. U. S. A. 78 (11), 6858–6862.

Aukrust, P., Svardal, A.M., Muller, F., Lunden, B., Berge, R.K., Ueland, P.M., Froland, S.S., 1995. Increased levels of oxidized glutathione in CD4+ lymphocytes associated with disturbed intracellular redox balance in human immunodeficiency virus type 1 infection. Blood 86, 258–267.

Bache, S.E., Maclean, M., MacGregor, S.J., Anderson, J.G., Gettinby, G., Coia, J.E., Taggart, I., 2012. Clinical studies of the HINS-light environmental decontamination system for continuous disinfection in the burn unit inpatient and outpatient settings. Burns 38, 69–76.

Brubacher, J.L., Bols, N.C., 2001. Chemically de-acetylated 2′,7′-dichlorodihydrofluorescein diacetate as a probe of respiratory burst activity in mononuclear phagocytes. J. Immunol. Methods 251 (1–2), 81–91.

Bruck, R., Shirin, H., Aeed, H., Matas, Z., Hochman, A., Pines, M., Avni, Y., 2001. Prevention of hepatic cirrhosis in rats by hydroxyl radical scavengers. J. Hepatol. 35 (4), 457–464.

Carelli, S., Ceriotti, A., Cabibbo, A., Fassina, G., Ruvo, M., Sitia, R., 1997. Cysteine and glutathione secretion in response to protein disulfide bond formation in the ER. Science 277, 1681–1684.

Chiaviello, A., Postiglione, I., Palumbo, G., 2011. Targets and mechanisms of photodynamic therapy in lung cancer cells: a brief overview. Cancers 3 (1), 1014–1041.

Cogen, A.L., Nizet, V., Gallo, R.L., 2008. Skin microbiota: a source of disease or defence? Br. J. Dermatol. 158 (3), 442–455.

Dai, T., Gupta, A., Huang, Y.Y., Yin, R., Murray, C.K., Vrahas, M.S., Sherwood, M.E., Tegos, G.P., Hamblin, M.R., 2013. Blue light rescues mice from potentially fatal *Pseudomonas aeruginosa* burn infection: efficacy, safety and mechanism of action. Antimicrob. Agents Chemother. 57, 1238–1245.

Desagher, S., Glowinski, J., Prémont, J., 1997. Pyruvate protects neurons against hydrogen peroxide-induced toxicity. J. Neurosci. 17 (23), 9060–9067.

Devasagayam, T.P.A., Tilak, J.C., Boloor, K.K., Sane, K.S., Ghaskadbi, S.S., Lele, R.D., 2004. Free radicals and antioxidants in human health: current status and future prospects. J. Assoc. Physicians India 52, 796.

Engelmann, J., Volk, J., Leyhausen, G., Geurtsen, W., 2005. ROS formation and glutathione levels in human oral fibroblasts exposed to TEGDMA and camphorquinone. J. Biomed. Mater. Res. B Appl. Biomater. 75 (2), 272–276.

Faraci, F.M., Didion, S.P., 2004. Vascular protection: superoxide dismutase isoforms in the vessel wall. Arterioscler. Thromb. Vasc. Biol. 24 (8), 1367–1373.

Gayl, S.V., 2001. Photofrin-mediated photodynamic therapy for treatment of aggressive head and neck nonmelanomatous skin tumors in elderly patients. Laryngoscope 111 (6), 1091–1098.

Hissin, P.J., Hilf, P.R., 1976. A fluorometric method for determination of oxidized and reduced glutathione in tissues. Anal. Biochem. 74 (1), 214–226.

Ho, G., Grant, M.H., Barbenel, J.C., Henderson, C.J., 2004. Low-level laser therapy on tissue-engineered skin substitutes: effect on the proliferation rate of 3 T3 mouse fibroblast cells. Proc. SPIE 5610, 124–134.

Hockberger, P.E., Skimina, T.A., Centonze, V.E., Lavin, C., Chu, S., Dadras, S., Reddy, J.K., White, J.G., 1999. Activation of flavin-containing oxidases underlies light-induced production of H_2O_2 in mammalian cells. Proc. Natl. Acad. Sci. U. S. A. 96 (11), 6255–6260.

Hwan, K.S., Lee, H.S., Ryu, D.S., Choi, S.J., Lee, D.S., 2011. Antibacterial activity of silver-nanoparticles against *Staphylococcus aureus* and *Escherichia coli*. Korean J. Microbiol. Biotechnol. 39 (1), 77–85.

Johnson, I., Spence, M.T.Z., 2010. Molecular probes handbook, a guide to fluorescent probes and labeling technologies. Chapter 18 — Probes for Reactive Oxygen Species, Including Nitric Oxide, 11th ed., pp. 815–817.

Jung, I.L., Oh, T.J., Kim, I.G., 2003. Abnormal growth of polyamine-deficient *Escherichia coli* mutant is partially caused by oxidative stress-induced damage. Arch. Biochem. Biophys. 418 (2), 125–132.

Kotelevets, L.M., Babenko, Iu.S., Lukoianova, M.A., 1988. Spectral properties of cytochromes from *Staphylococcus aureus*. Prikl. Biokhim. Mikrobiol. 24 (1), 68–75.

Lavi, R., Sinyakov, M., Samuni, A., Shatz, S., Friedmann, H., Shainberg, A., Breitbart, H., Lubart, R., 2004. ESR detection of $_1O^2$ reveals enhanced redox activity in illuminated cell cultures. Free Radic. Res. 38 (9), 893–902.

Li, Y., Huang, T.T., Carlson, E.J., Melov, S., Ursell, P.C., Olson, J.L., Noble, L.J., Yoshimura, M.P., Berger, C., Chan, P.H., Wallace, D.C., Epstein, C.J., 1995. Dilated cardiomyopathy and neonatal lethality in mutant mice lacking manganese superoxide dismutase. Nat. Genet. 11 (4), 376–381.

Linas, S.L., Shanley, P.F., White, C.W., Parker, N.P., Repine, J.E., 1987. O_2 metabolite-mediated injury in perfused kidneys is reflected by consumption of DMTU and glutathione. Am. J. Physiol. 253 (4 Pt 2), F692–F701.

Locigno, R., Castronovo, V., 2001. Reduced glutathione system: role in cancer development, prevention and treatment (review). Int. J. Oncol. 19, 221–236.

Lowry, O.H., Rosebrough, N.J., Farr, A.L., Randall, R.J., 1951. Protein measurement with the folin phenol reagent. J. Biol. Chem 193 (1), 265–275.

Lubart, R., Lipovski, A., Nitzan, Y., Friedmann, H., 2011. A possible mechanism for the bactericidal effect of visible light. Laser Ther. 20 (1), 17–22.

Maclean, M., MacGregor, S.J., Anderson, J.G., Woolsey, G.A., 2008. The role of oxygen in the visible-light inactivation of Staphylococcus aureus. J Photochem Photobiol B. 92 (3), 180–184.

Maclean, M., MacGregor, S.J., Anderson, J.G., Woolsey, G.A., 2009. Inactivation of bacterial pathogens following exposure to light from a 405-nm LED array. Appl. Environ. Microbiol. 75 (7), 1932–1937.

Maclean, M., Macgregor, S.J., Anderson, J.G., Woolsey, G.A., Coia, J.E., Hamilton, K., Taggart, I., Watson, S.B., Thakker, B., Gettinby, G., 2010. Environmental decontamination of a hospital isolation room using high-intensity narrow-spectrum light. J. Hosp. Infect. 76 (3), 247–251.

Maclean, M., Murdoch, L.E., MacGregor, S.J., Anderson, J.G., 2013. Sporicidal effects of high intensity 405 nm visible light on endospore-forming bacteria. Photochem. Photobiol. 89, 120–126.

Maclean, M., McKenzie, K., Anderson, J.A., Gettinby, G., MacGregor, S.J., 2015. 405 nm light technology for the inactivation of pathogens and its potential role for environmental disinfection and infection control. J. Hosp. Infect. 88 (1), 1–11.

McDonald, R.S., Grant, M.H., MacGregor, S.J., Anderson, J.G., Maclean, M., 2011. Effect of 405 nm high-intensity narrow-spectrum light on fibroblast populated collagen lattices: an in vitro model of wound healing. J. Biomed. Opt. 16 (4), 048003.

McDonald, R.S., Gupta, S., Maclean, M., Ramakrishnan, P., Anderson, J.G., MacGregor, S.J., Meek, R.M., Grant, M.H., 2013. 405 nm light exposure of osteoblasts and inactivation of bacterial isolates from arthroplasty patients: potential for new disinfection applications? Eur. Cell. Mater. 25, 204–214.

McKenzie, K., Maclean, M., Timoshkin, I.V., MacGregor, S.J., Anderson, J.G., 2014. Enhanced 311 inactivation of *Escherishia coli* and *Listeria monocytogenes* by exposure to 405 nm light under sub lethal temperature, salt and acid stress conditions. Int. J. Food Microbiol. 170, 91–98.

Meriga, B., Reddy, B.K., Rao, K.R., Reddy, L.A., Kishor, P.B.K., 2004. Aluminium-induced production of oxygen radicals, lipid peroxidation and DNA damage in seedlings of rice (*Oryza sativa*). J. Plant Physiol. 161 (1), 63–68.

Mittler, R., 2002. Oxidative stress, antioxidants and stress tolerance. Trends Plant Sci. 7 (9), 405–410.

Noctor, G., Foyer, C.H., 1998. Ascorbate and glutathione: keeping active oxygen under control. Annu. Rev. Plant Physiol. Plant Mol. Biol. 49, 249–279.

Otto, M., 2009. *Staphylococcus epidermidis*—the 'accidental' pathogen. Nat. Rev. Microbiol. 7 (8), 555–567.

Packer, L., Weber, S.U., Rimbach, G., 2001. Molecular aspects of α-tocotrienol antioxidant action and cell signalling. J. Nutr. 131 (2), 369S–373S.

Padayatty, S.J., Katz, A., Wang, Y., Eck, P., Kwon, O., Lee, J.H., Chen, S., Corpe, C., Dutta, A., Dutta, S.K., Levine, M., 2003. Vitamin C as an antioxidant: evaluation of its role in disease prevention. J. Am. Coll. Nutr. 22 (1), 18–35.

Pattison, D.I., Davies, M., 2006. Actions of ultraviolet light on cellular structures. EXS (96), 131–157.

Pompella, A., Visvikis, A., Paolicchi, A., Tata, V., Casini, A.F., 2003. The changing faces of glutathione, a cellular protagonist. Biochem. Pharmacol. 66 (8), 1499–1503.

Ramakrishnan, P., Maclean, M., MacGregor, S.J., Anderson, J.G., Grant, M.H., 2014. Differential sensitivity of osteoblasts and bacterial pathogens to 405-nm light highlighting potential for decontamination applications in orthopedic surgery. J. Biomed. Opt. 19 (10), 105001.

Rappeneau, S., Baeza-Squiban, A., Marano, F., Calvet, J., 2000. Efficient protection of human bronchial epithelial cells against sulfur and nitrogen mustard cytotoxicity using drug combinations. Toxicol. Sci. 58 (1), 153–160.

Schimmel, M., Bauer, G., 2002. Proapoptotic and redox state-related signalling of reactive oxygen species generated by transformed fibroblasts. Oncogene 21 (38), 5886–5896.

Shah, K., Kumar, R.G., Verma, S., Dubey, R.S., 2001. Effect of cadmium on lipid peroxidation, superoxide anion generation and activities of antioxidant enzymes in growing rice seedlings. Plant Sci. 161 (6), 1135–1144.

Sharma, P., Dubey, R.S., 2005. Drought induces oxidative stress and enhances the activities of antioxidant enzymes in growing rice seedlings. Plant Growth Regul. 46 (3), 209–221.

Sies, H., 1997. Oxidative stress: oxidants and antioxidants. Exp. Physiol. 82 (2), 291–295.

Smith, M.D., Barbenel, J.C., Courtney, J.M., Grant, M.H., 1992. Novel quantitative methods for the determination of biomaterial cytotoxicity. Int. J. Artif. Organs 15, 73–76.

Tanaka, Y., Tran, P.O., Harmon, J., Robertson, R.P., 2002. A role for glutathione peroxidase in protecting pancreatic beta cells against oxidative stress in a model of glucose toxicity. Proc. Natl. Acad. Sci. U. S. A. 99 (19), 12363–12368.

Testa, M.P., Alvarado, O., Wournell, A., Lee, J., Guilford, F.T., Henriksen, S.H., Phillips, T.R., 2011. Screening assay for oxidative stress in a feline astrocyte cell line, G355-5. J. Vis. Exp. 53, e2841.

Townsend, D.M., Tew, K.D., Tapiero, H., 2003. The importance of glutathione in human disease. Biomed. Pharmacother. 57, 145–155.

Trifunovic, A., Hansson, A., Wredenberg, A., Rovio, A.T., Dufour, E., Khvorostov, I., Spelbrink, J.N., Wibom, R., Jacobs, H.T., Larsson, N.G., 2005. Somatic mtDNA mutations cause aging phenotypes without affecting reactive oxygen species production. Proc. Natl. Acad. Sci. U. S. A. 102 (50), 17993–17998.

Wang, X., Perez, E., Liu, R., Yan, L.J., Mallet, R.T., Yang, S.H., 2007. Pyruvate protects mitochondria from oxidative stress in human neuroblastoma SK-N-SH cells. Brain Res. 1132 (1), 1–9.

Waugh, D.G., Lawrence, J., 2013. Laser Surface Treatment of a Polymeric Biomaterial: Wettability Characteristics and Osteoblast Cell Response Modulation. vol. 1. Old city Publishing, Philadelphia, PA, p. 216.

Wu, D., Yotnda, P., 2011. Production and detection of reactive oxygen species (ROS) in cancers. J. Vis. Exp. 57, 3357.

Zhang, Y., Zhu, Y., Gupta, A., Huang, Y., Muuay, C.K., Vrahas, M.A., Sherwood, M.E., Baer, D.G., Hamblin, M.R., Dai, T., 2014. Antimicrobial blue light therapy for multi-drug resistant *Acinetobacter baumanni* infection in mice: implications for prophylaxis and treatment of combat related infection. J. Infect. Dis. 17, 122–127.